Supporting Information: Limits for Recombination in a Low Energy Loss Organic Heterojunction

S. Matthew Menke[1], Aditya Sadhanala[1], Mark Nikolka[1], Niva A. Ran[2], Mahesh Kumar Ravva[3], Safwat Abdel-Azeim[3], Hannah L. Stern[1], Ming Wang[2], Henning Sirringhaus[1], Thuc-Quyen Nguyen[2], Jean-Luc Brédas[3], Guillermo C. Bazan[2], and Richard H. Friend[1]*

[1]SMM, AS, HLS, MN, HS, and RHF
Department of Physics, Cavendish Laboratory, University of Cambridge, J.J. Thompson Avenue, Cambridge, CB3 0HE, United Kingdom
[*]Corresponding Author: rhf10@cam.ac.uk

[2]NAR, MW, TQN, and GCB
Center for Polymers and Organic Solids, University of California, Santa Barbara, Santa Barbara, CA, 93106, USA

[3]MKR, SAA, JLB
KAUST Solar Center, Division of Physical Science and Engineering, King Abdullah University of Science and Technology, Thuwal 23955-6900, Saudi Arabia

Contents:

1. TD-DFT Calculations for S_1 and E_{CT} excitation energies

A large number of configurations were generated for the PIPCP-$PC_{61}BM$ complex at the DFT ωB97XD/6-31G(d,p) level of theory. We emphasize that a long-range corrected functional with consideration of dispersion interactions such as ωB97XD can provide a reliable description of the extent of the wavefunction delocalization along the π-conjugated backbone and of the intermolecular interactions exist between polymer and fullerene. We have used a PIPCP oligomer consisting of one IDT, one CPDT, and two PT units, capped on both ends by a thiophene ring (Fig. S1); such an oligomer chain length allows complete delocalization of the hole wavefunction; the alkyl side-chains were replaced with methyl groups to minimize computational costs. We have generated randomly up to eight PIPCP-$PC_{61}BM$ complexes by considering the $PC_{61}BM$ molecule at different locations around the PIPCP backbone. Then, TD-DFT/PCM calculations were performed (at the ωB97XD/6-31G(d,p) level) to predict the energy for singlet excitons (S_1) and charge transfer states (E_{CT}) in PIPCP:$PC_{61}BM$ complexes.

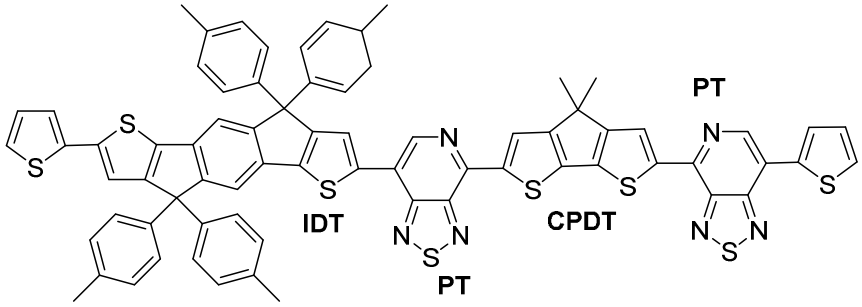

Figure S1. Chemical structure of the PIPCP model oligomer considered in our calculations.

The calculations firstly show that the red-shift in absorption for PIPCP between the pure and blend films cannot be solely attributed to a change in the dielectric constant. Such would be the case if the morphology of blend films leads to a locally larger dielectric constant. Table S1 shows the energies for S_1 calculated using dielectric constants between 3.5–5. It is clear that a

change in the dielectric constant does not change S_1 to any appreciable extent and therefore other factors must be contributing to the 60 meV red-shifted absorption in PIPCP:$PC_{61}BM$ blend films.

Table S1 | Singlet Exciton Energies (S_1) for PIPCP as a function of dielectric constant

Relative Dielectric Constant	S_1 Excitation Energies (eV)
3.5	1.62
4.0	1.62
4.5	1.63
5.0	1.63

In order to describe the E_{CT} between PIPCP and $PC_{61}BM$, TD-DFT calculations were performed on the basis of the ground-state geometries. The energies for S_1 and E_{CT} are shown in Table S2. For the eight configurations of the PIPCP-$PC_{61}BM$ complexes, the average difference between the nominally local S_1 excitation of the backbone and E_{CT} is ca. 0.1 eV. Importantly, however, a natural transition orbital (NTO) analysis points to the appearance of states with hybrid Frenkel-CT character, where the electron wavefunction in these lowest two excited states of the complex delocalizes over both the PIPCP backbone and $PC_{61}BM$ (see Figure S2 for configuration 1). In the lowest excited state (labelled CT in Figure S2 and Table S2), the electron-NTO appears mainly on the fullerene with a partial delocalization on the PIPCP, which results in a significant oscillator strength; these characteristics are reversed in the second lowest excited state (labelled S_1 in Figure S2 and Table S2), which results in a higher oscillator strength.

Finally, it is interesting to note that, in the case of configurations 6-8, the nature of the PIPCP oligomer – fullerene interactions is such that the characteristics of the hybrid Frenkel-CT states are reversed, with stronger Frenkel character in the lowest excited state.

Table S2 | Singlet Intramolecular Exciton (S_1) and Charge Transfer (E_{CT}) Energies for the various PIPCP:$PC_{61}BM$ configurations. Oscillator strengths (in atomic units) are given in parentheses. The isolated PIPCP singlet exciton energy is also given for the sake of comparison.

Configuration	E_{CT} (eV)	S_1 (eV)
Isolated PIPCP		1.62 (1.835)
1	1.52 (0.396)	1.66 (1.135)
2	1.59 (0.025)	1.67 (1.466)
3	1.55 (0.597)	1.61 (0.526)
4	1.57 (0.679)	1.59 (0.548)
5	1.51 (0.172)	1.66 (1.056)
6	1.67 (0.168)	1.58 (1.246)
7	1.73 (0.148)	1.68 (1.322)
8	1.73 (0.367)	1.64 (1.142)

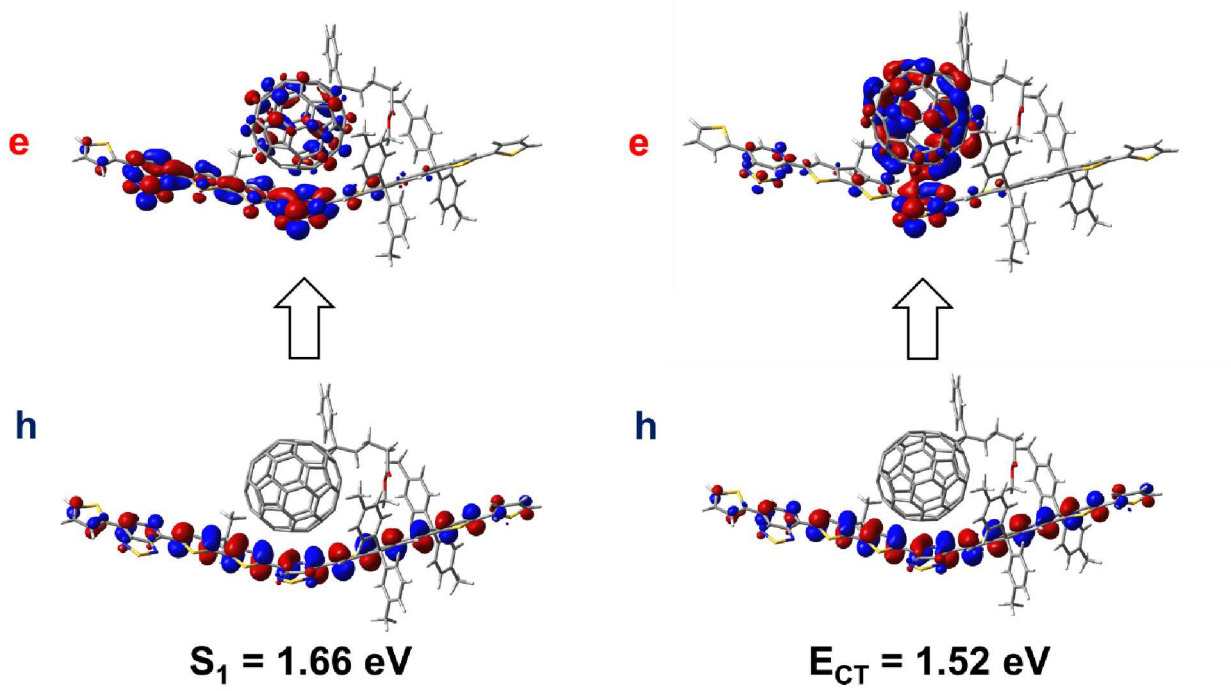

Figure S2. Calculated excitation energies and illustration of the natural transition orbitals (h: hole; e: electron) for the $^1CT_1$ and S1 states of configuration 1 in Table S2, at the TD-ωB97XD/6-31G(d,p) level coupled with the PCM model (isovalue surface corresponding to 0.02 atomic units).

2. Broadband transient absorption spectra for PIPCP:$PC_{61}BM$ blend films

Figure S3 shows the transient absorption (TA) spectra for a PIPCP:$PC_{61}BM$ blend film from 0.5ps to 60ps measured at an excitation wavelength of λ_{ex}=600 nm and moderate excitation fluence of 3 μJcm^{-2}. The region of the ground state bleach is located between 700–850 nm, in agreement with the steady-state absorption. Negative features indicated photoinduced absorption of excited states within the blend. Note that no spectral signature for electroabsorption can be seen in the wavelength region between 850–950 nm.

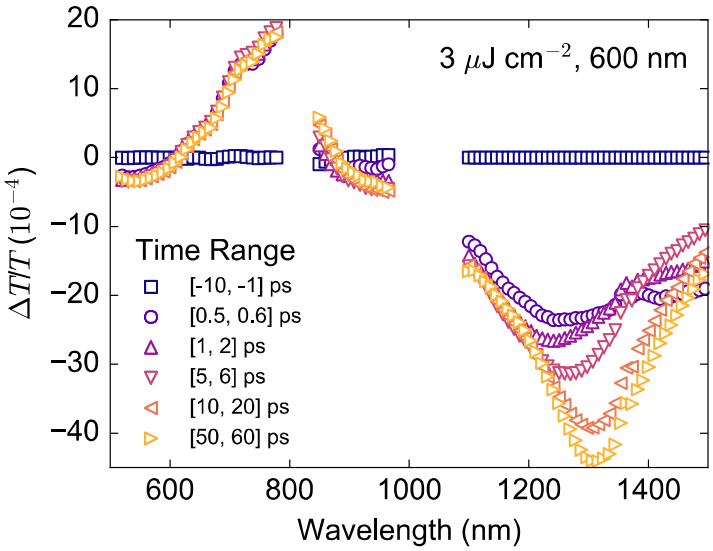

Figure S3. Transient absorption spectra for a PIPCP:$PC_{61}BM$ blend film for various times ranges between 0.5 and 60 ps measured at an excitation wavelength of λ_{ex}=600 nm and excitation fluence of 3 μJcm^{-2}.

3. Extracted charge and triplet kinetics from 1ns to 1µs

Figure S4 shows the extracted charge and triplet kinetics for a range of fluences between 0.4–10 µJcm^{-2} at an excitation wavelength of λ_{ex}=532 nm. The solid lines reflect the fitting of the triplet kinetics according to Eq. 3 in the main text. As was shown for the shorter timescale measurements, the decay of charges occurs more rapidly at higher fluences and the onset of triplet formation occurs at shorter times at higher fluences. Both of these are in agreement with bimolecular charge decay and triplet formation.

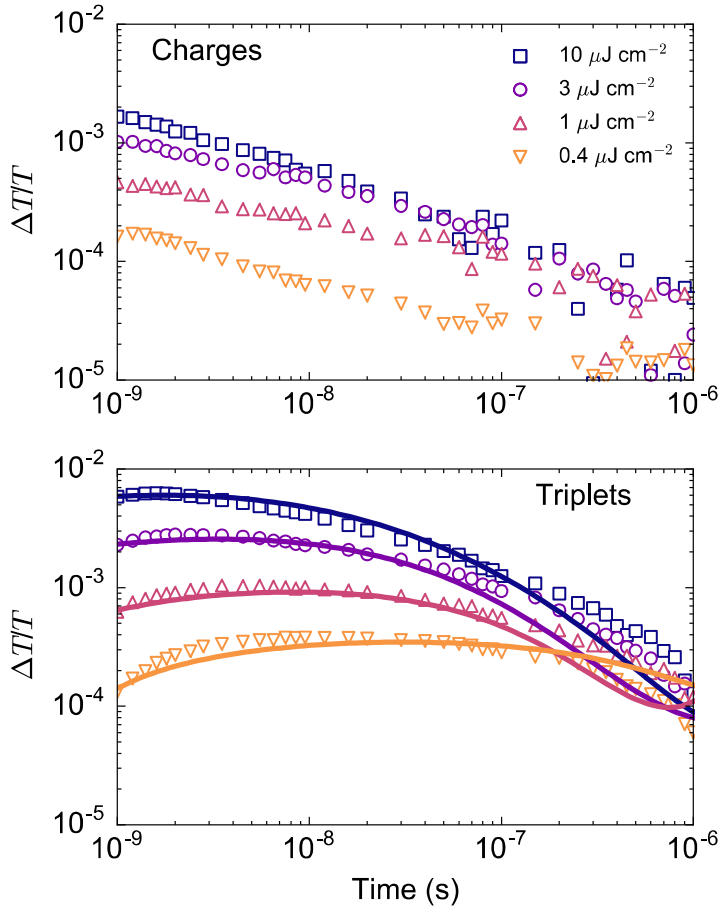

Figure S4. Extracted kinetics for charges and triplet excitons in a PIPCP:$PC_{61}BM$ blend between 1ns and 1µs.

4. Confirmation of triplet photoinduced absorption spectrum

In order to confirm that the new spectral feature that appears in the photoinduced absorption spectra is indeed that of a triplet exciton on the PIPCP polymer, transient absorption measurements were carried out on a film containing 5 wt.% PIPCP, 5 wt.% Pt octaethylporphyrin (PtOEP) diluted in polystyrene (PS). Under an illumination at λ_{ex}=532 nm, singlet excitons formed on PtOEP can convert to triplet excitons owing to a large degree of spin-orbit coupling. As the energy of a triplet exciton on PtOEP is approximately 1.9 eV, energy transfer through the PS matrix results in the formatin of triplet excitons on PIPCP. Figure S5 compares the extracted triplet signature from PIPCP:$PC_{61}BM$ blends films with that extracted from the triplet sensitization scheme. The agreement in spectral position confirms that triplet excitons in PIPCP exhibit a peak in photoinduced absorption at approximately 1300 nm that is notably distinct for that of a polaron which peaks at approximately 1250 nm. The difference in spectral width may arise due to different polymer configurations achieved when blended with PS instead of $PC_{61}BM$.

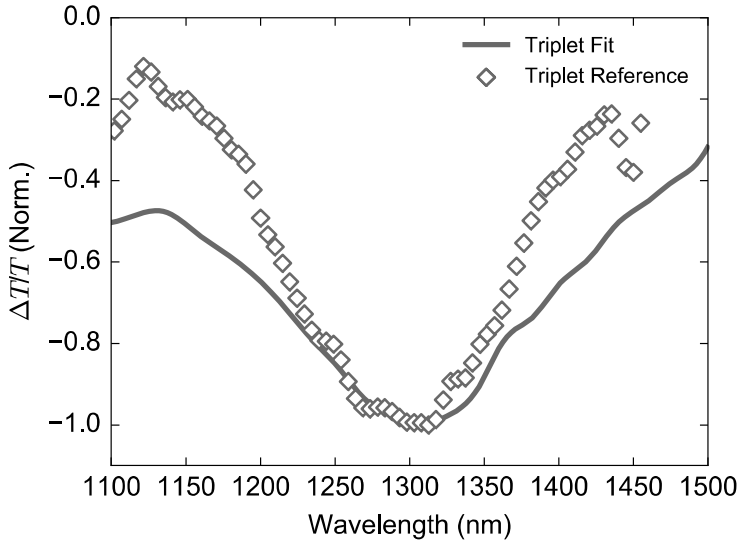

Figure S5. Normalized photoinduced absorption spectra for the triplet spectral feature extracted from the global analysis of PIPCP:$PC_{61}BM$ blends films (Triplet Fit) and the triplet spectral feature extracted from triplet sensitization experiments (Triplet Reference).

5. Output characteristics for the PIPCP:$PC_{61}BM$ blend films

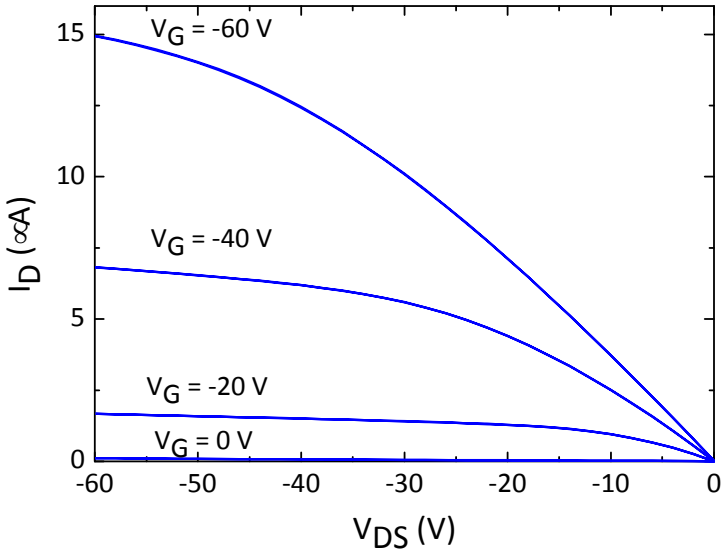

Figure S6. Output characteristics for PIPCP:$PC_{61}BM$ blend films as a function drain-source voltage for gate voltages between 0V to -60V.

6. Temperature dependent mobility measurements for pure PIPCP films

Figure S7 shows the field effect hole mobility (μ_{FET}) for films of pure PIPCP as a function of temperature between 200–300K. Descriptions of the measurement can be found in the manuscript. Note that in contrast to the PIPCP:$PC_{61}BM$ blends, films of pure PIPCP show a notable degree of gate voltage dependent hole mobility near room temperature. The gate voltage dependence becomes weaker at lower temperatures and is likely caused by poor injection, making difficult the determination of an intrinsic mobililty from this measurement.

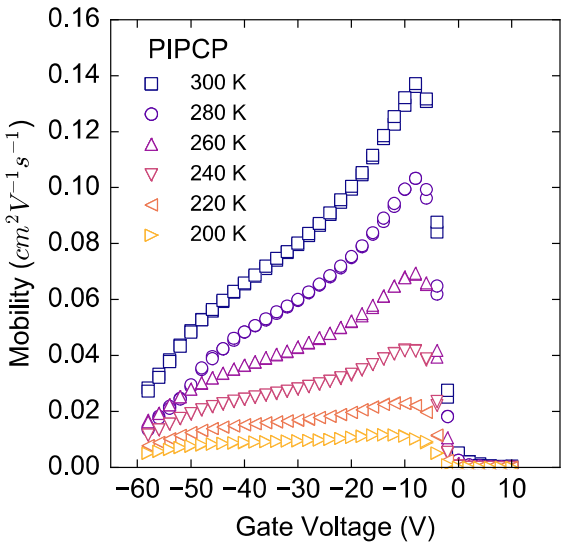

Figure S7. Field effect mobility of pure PIPCP films as a function of gate voltage for temperatures between 200–300K.

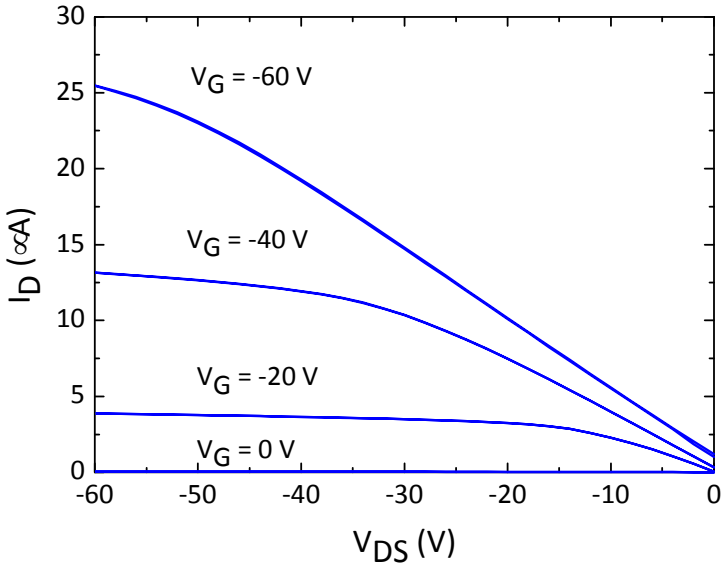

Figure S8. Output characteristics for pure PIPCP films as a function drain-source voltage for gate voltages between 0V to -60V.